



Title	Redox reactions of small organic molecules using ball milling and piezoelectric materials
Author(s)	Kubota, Koji; Pang, Yadong; Miura, Akira; Ito, Hajime
Citation	Science, 366(6472), 1500-1504 https://doi.org/10.1126/science.aay8224
Issue Date	2019-12-20
Doc URL	http://hdl.handle.net/2115/76621
Rights	This is the author ' s version of the work. It is posted here by permission of the AAAS for personal use, not for redistribution. The definitive version was published in Science on Volume 366 number 6472, 2019-12-20, DOI: 10.1126/science.aay8224.
Type	article (author version)
File Information	revised manuscript.pdf



[Instructions for use](#)

Redox Reactions of Small Organic Molecules Using Ball Milling and Piezoelectric Materials

Koji Kubota^{1,2*}, Yadong Pang², Akira Miura², Hajime Ito^{1,2*}

5 **Affiliations:**

¹Institute for Chemical Reaction Design and Discovery (WPI-ICReDD), Hokkaido University, Sapporo, Hokkaido 060-8628, Japan.

²Division of Applied Chemistry, Graduate School of Engineering, Hokkaido University, Sapporo, Hokkaido 060-8628, Japan.

10 *Correspondence to: hajito@eng.hokudai.ac.jp (H.I.), kbt@eng.hokudai.ac.jp (K.K.)

Abstract: Over the past decade, photoredox catalysis has harnessed light energy to accelerate bond-forming reactions. We postulated that a complementary method for the redox-activation of small organic molecules in response to applied mechanical energy could be developed through the piezoelectric effect. Here, we report that agitation of piezoelectric materials via ball milling reduces aryl diazonium salts. This mechanoredox system can be applied to arylation and borylation reactions under mechanochemical conditions.

One Sentence Summary: The first examples of arylation and borylation reactions using mechanically induced piezoelectricity have been developed.

Main Text: Visible-light photoredox catalysis represents a key recent development in contemporary organic synthesis (1–5). In these transformations, the photoexcited catalyst can act as a potent single-electron oxidant, transferring an electron to an acceptor (**A**), after which single-electron oxidation of a donor (**D**) affords the product under concomitant regeneration of the ground state catalyst (Fig. 1A). The broad success of photoredox catalysis hinges on the susceptibility of the coupling partners to redox activation and ensuing bond-forming reactions with high levels of efficiency and selectivity.

There has likewise been substantial parallel progress in mechanochemical organic transformations using ball milling (6–18). Since the term mechanochemistry was introduced by Ostwald in 1887, mechanochemical synthesis has been extensively exploited in materials science (6–8), polymer chemistry (9), and inorganic synthesis (8), but its application to organic synthesis is more recent (10–18). Advantages of the approach include the avoidance of potentially harmful organic solvents and external heating, shorter reaction times, and simpler operational handling. In addition, mechanochemical reactions are particularly useful for substrates that are poorly soluble in common organic solvents.

Inspired by the unique profile of photoredox systems based on light irradiation and the utility of ball milling in mechanochemistry, we hypothesized that redox activation of small organic molecules could be achieved through a mechanistically distinct approach using mechanical energy

(19–22). In particular, we envisioned that the agitation of piezoelectric materials (23–35) via ball milling could generate temporarily highly polarized particles that might act as strong reductants to transfer electrons to small organic molecules, followed by oxidative quenching of a donor, thus inducing the selective formation of bonds in a manner analogous to photoredox catalysis (Fig. 1B). Such a mechanoredox approach could potentially represent a powerful and attractive strategy to reduce the environmental impact of chemical processes; photoredox approaches, similar to other conventional organic reactions, often require complicated reaction set-ups, substantial amounts of dry and degassed organic solvents as well as an inert gas atmosphere (1–5).

For a proof-of-concept study, we selected commercially available, inexpensive, and easy-to-handle BaTiO₃ nanoparticles as the piezoelectric material (Fig. 1B). This choice was motivated by pioneering studies, in which ultrasonic agitation of BaTiO₃ produces a suitable electrochemical potential to overcome the water splitting potential (1.23 V) (28, 29) and reduce a *N,N,N',N',N'',N''*-hexamethyl[tris(aminoethyl)amine] (Me₆TREN)-ligated CuBr₂ complex, which has a reduction potential of –0.30 V (vs. SCE) (29, 36). These studies suggested that mechanical agitation of BaTiO₃ in a ball mill could generate an electrochemical potential suitable for the activation of redox-active small organic molecules in organic synthesis.

The photoredox systems that activate aryl diazonium salts for coupling with heteroarenes (37) or borylation (38) have been reported by König and Yan, respectively. The key step in these transformations is the photochemical reduction of aryl diazonium salts to aryl radical species. Andrieux and Pinson have reported a reduction potential of –0.16 V (vs. SCE) for phenyl diazonium tetrafluoroborate (39), which was within range for feasible redox activation using BaTiO₃. In our postulated mechanism (Fig. 1C), the agitation of BaTiO₃ via ball milling generates a temporary electrochemical potential in response to mechanical impact. According to the aforementioned inorganic studies (28, 29), the temporary polarization should be sufficiently persistent to reduce an aryl diazonium salt (**1**) via a SET mechanism analogous to the photoredox reaction, to furnish the corresponding aryl radical **I**. The addition of **I** to heteroarene **2** would afford radical addition intermediate **II**, which would be subsequently oxidized by the hole in the agitated BaTiO₃ to form carbocation intermediate **III** (37). Finally, deprotonation of **III** would lead to arylation product **3**. In the borylation (38), the generated radical **I** reacts with bis(pinacolate)diboron (**4**), to cleave the B–B bond, resulting in the formation of the boryl substitution product **5** as well as radical anion intermediate **IV**. Subsequently, oxidation of **IV** by the agitated BaTiO₃ could form F–B(pin) (**V**) as a byproduct.

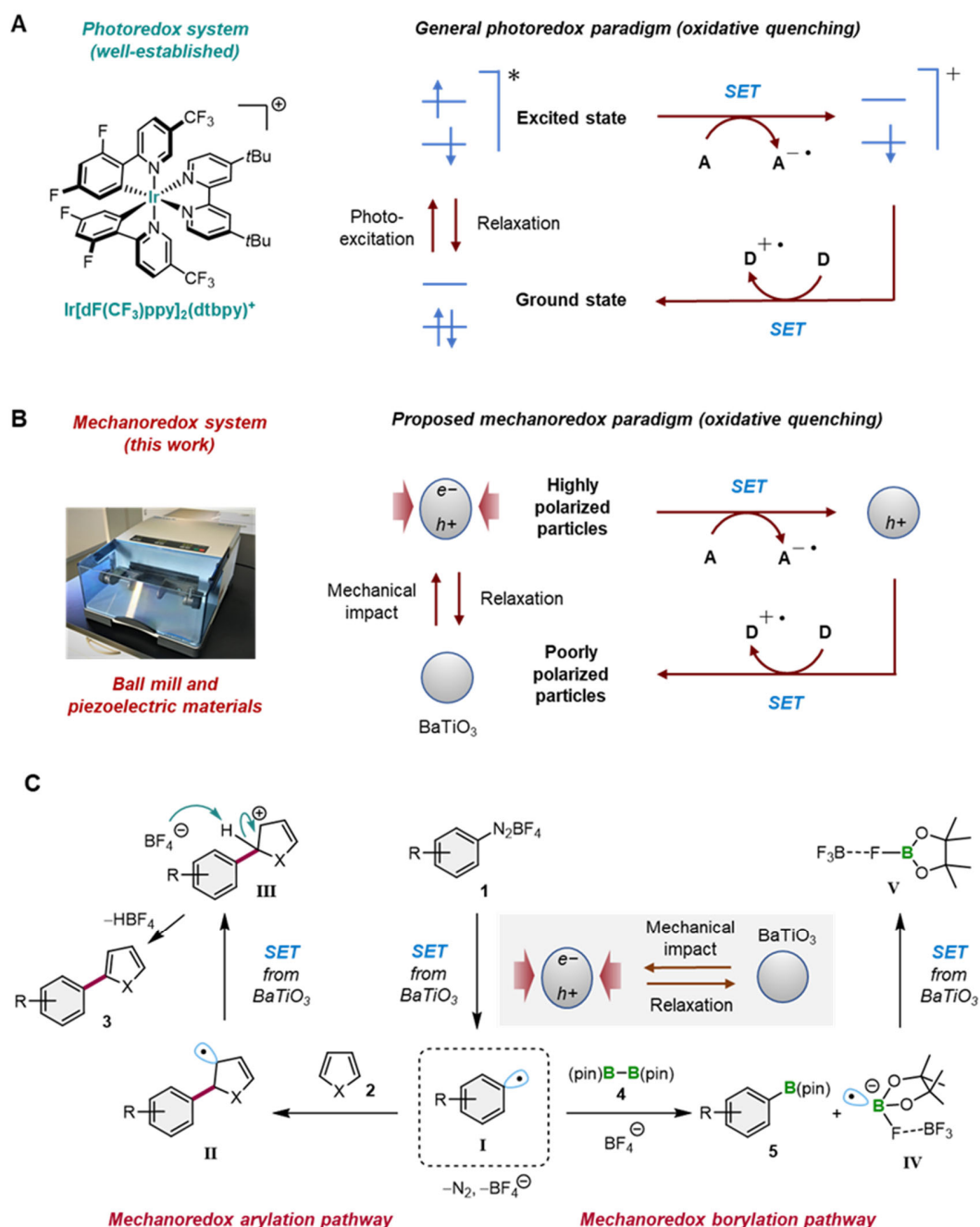


Fig. 1. Working hypothesis for a mechano-redox system for the activation of small organic molecules in organic synthesis. (A) A commonly employed photoredox catalyst and a generic photoredox oxidative quenching cycle. (B) Proposed mechano-redox paradigm using a ball mill and a piezoelectric material. (C) Proposed mechanism for the mechano-redox arylation and borylation using BaTiO₃ and ball milling. SET: single-electron transfer.

To explore this mechanistic hypothesis, we first attempted the proposed mechano-redox C–H arylation with **1a** and furan (**2a**) in the presence of commercially available BaTiO₃ using a

Retch MM400 mixer mill (1.5 mL stainless-steel milling jar with 5-mm diameter stainless-steel ball) (Fig. 2A). The corresponding arylation product (**3a**) was obtained in 40% yield after milling at 20 Hz for 1 h under air. The reaction did not proceed in the absence of BaTiO₃, suggesting that the mechanical energy provided by ball milling generated the piezoelectric potential to reduce **1a**. In contrast, even when ultrasound irradiation was applied to the mixture with BaTiO₃ in dimethyl sulfoxide (DMSO) under a nitrogen atmosphere, the formation of the product was not observed. A small amount of **3a** was obtained when the reaction was carried out in the presence of SrTiO₃, which exhibits piezoelectric properties upon applying in-plane strain (40). When using non-piezoelectric ceramic materials, such as TiO₂, BaCO₃, or Al₂O₃, the reaction did not proceed, which suggests that piezoelectric materials are essential for this arylation reaction. We found that conducting the reaction at higher ball-milling frequency (30 Hz) significantly improved the yield (81%). This result is consistent with our hypothesis that the required piezoelectric potential is generated by mechanical force provided by the ball milling of BaTiO₃. Using other piezoelectric materials, such as LiNbO₃ and ZnO, also afforded **3a**, albeit in lower yield (24% and 15%, respectively). Using a bigger jar (5.0 mL) and ball (7.5 mm) provided **3a** in high yield (82%, Table S2). Product **3a** was isolated by filtration of the obtained crude solid mixture (Fig. 2B), followed by column chromatography on silica gel.

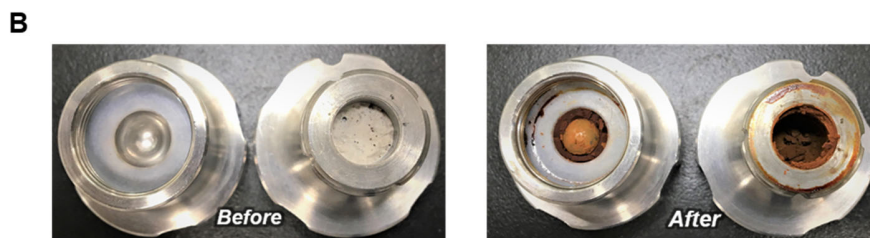
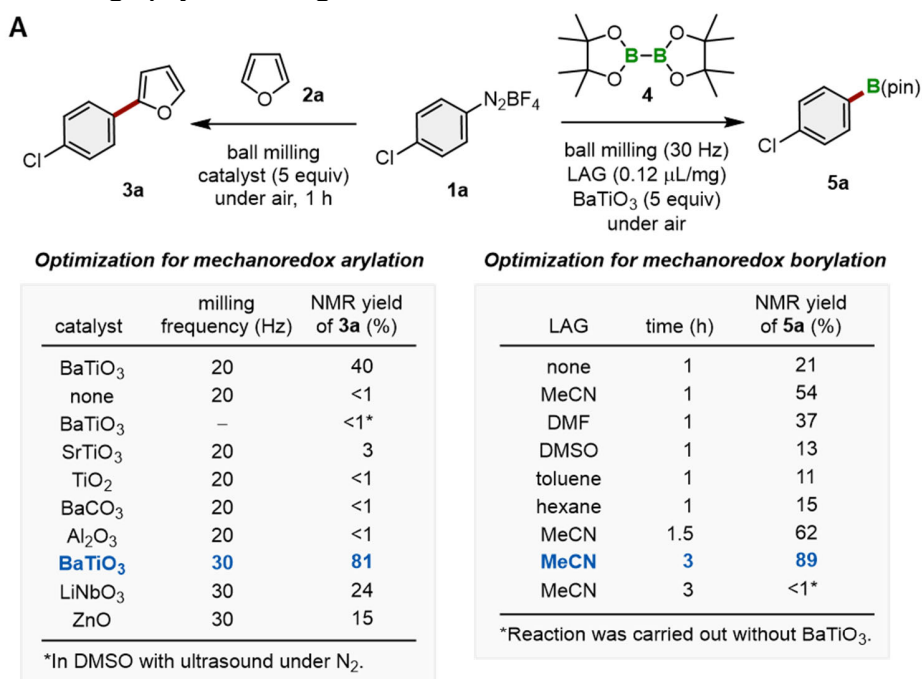


Fig. 2. Mechano-redox arylation and borylation using mechanical force. (A) Optimization of the mechano-redox arylation and borylation reactions. (B) Reaction mixture of the mechano-redox

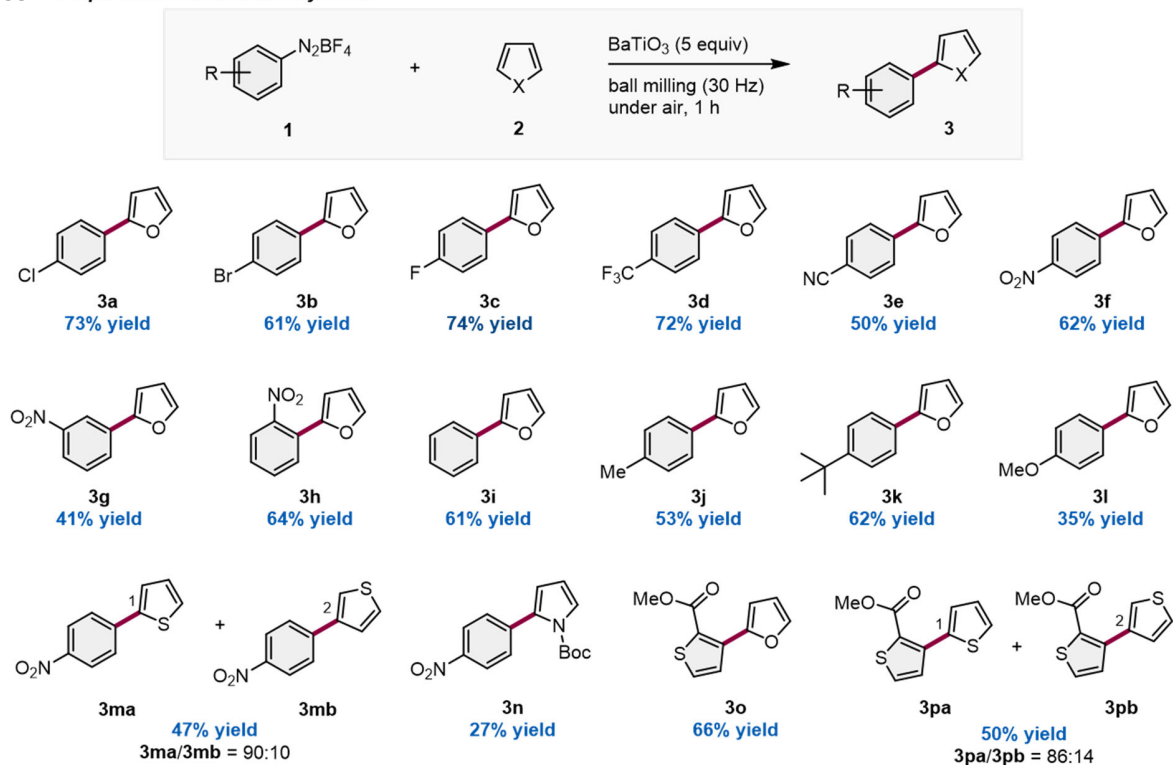
arylation of **2a** after grinding in a ball mill. A stainless-steel milling jar (1.5 mL) and a stainless-steel ball (diameter: 5 mm) were used. See supplementary materials for details.

5 We then investigated the possibility of mechano-redox borylation using the same setup (Fig. 2A). We found that the borylation of **1a** with **4** in the presence of BaTiO₃ afforded the desired arylboronate (**5a**) in 21% yield. Next, we attempted to improve the reactivity by using liquid-assisted-grinding (LAG), in which a substoichiometric amount of liquid is added (41). In all LAG reactions, the ratio of liquid additive (μL) to reactant (mg) was 0.12. Use of acetonitrile (MeCN) as the LAG additive improved the yield of **5a**, while other common solvents, such as *N,N*-dimethylformamide (DMF), DMSO, toluene, or hexane led to little or no improvement. We also found that prolonging the reaction time led to a higher yield of **3a** (89%) when MeCN was used as the LAG additive. Using a bigger jar (5.0 mL) and ball (7.5 mm) did not significantly affect the transformation (86%, Table S3). The reaction without BaTiO₃ did not proceed, supporting our mechanistic hypothesis. Compared with the analogous photoredox reaction, the present mechanoredox borylation exhibited much faster reaction kinetics and a better product yield (38).

15 Subsequently, we explored the scope of the mechanoredox arylation reaction with various aryl diazonium salts using a 5 mL stainless-steel milling jar with a 7.5-mm diameter stainless-steel ball (Fig. 3A). Electron-deficient aryl diazonium salts (**1a-1h**) were converted into the desired products (**3a-3h**) in good yield under the optimized conditions. Simple aromatic substrates (**1i-1k**) also reacted to give the corresponding products (**3i-3k**) in good yield. However, in the case of an electron-rich methoxy-substituted diazonium salt (**1l**), the product (**3l**) was obtained in relatively low yield. This was probably due to the relatively high reduction potential of **1l**. Other heteroarenes, namely, thiophene and pyrrole, successfully reacted to form the desired products (**3m** and **3n**). Arylation reactions using thienyl diazonium salts afforded the corresponding heterobiaryls (**3o** and **3p**), which are typical structural motifs for organic semiconductors (42). Minor regioisomers (**3mb** and **3pb**) were observed as competing products in the reactions with thiophene, whereas the photoredox system developed by König and co-workers, using Eosin Y, produced **3ma** and **3pa** as single isomers (37). We also confirmed that the developed mechanoredox borylation conditions were applicable to a variety of aryl diazonium salts (Fig. 3B).

20 25 30 35 To demonstrate the practical utility of this protocol, we investigated a gram-scale synthesis of heterobiaryls under the developed mechanoredox conditions, as well as the recycling of BaTiO₃ (Fig. 4A and 4B). The mechanoredox C–H arylation of furan (**2a**) with **1o** was carried out on a 8-mmol scale in a 25-mL stainless-steel ball-milling jar with one 15-mm diameter stainless steel ball, affording **3o** in 71% yield (Fig. 4A). After separation from the crude reaction mixture and washing, BaTiO₃ could be reused for the mechanoredox arylation of furan (**2a**) under the same reaction conditions at least three times before the yield of **3k** declined substantially (Fig. 4B).

A Scope of mechano-redox arylation



B Scope of mechano-redox borylation

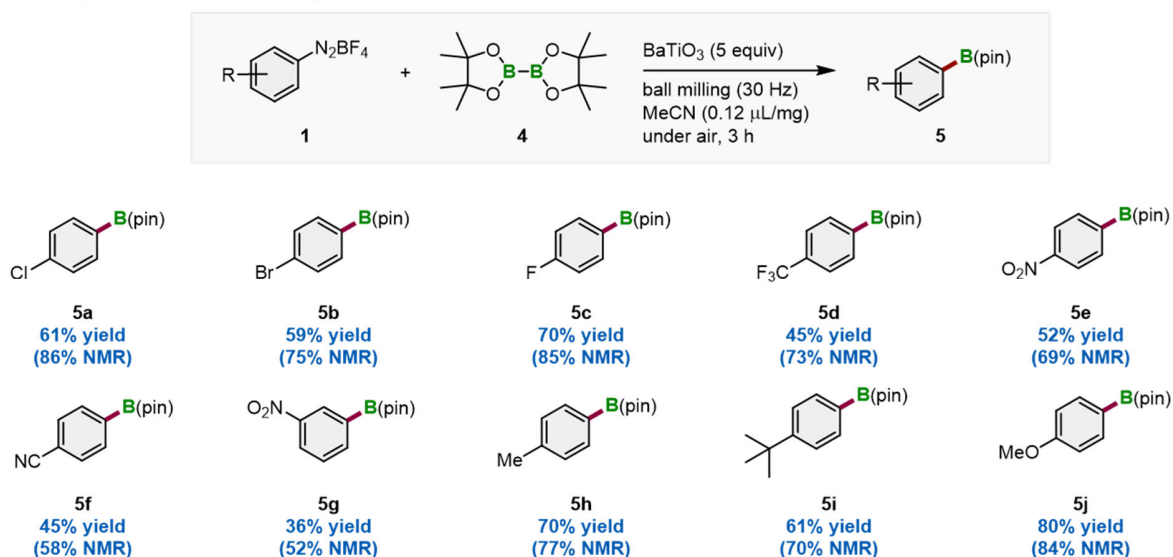
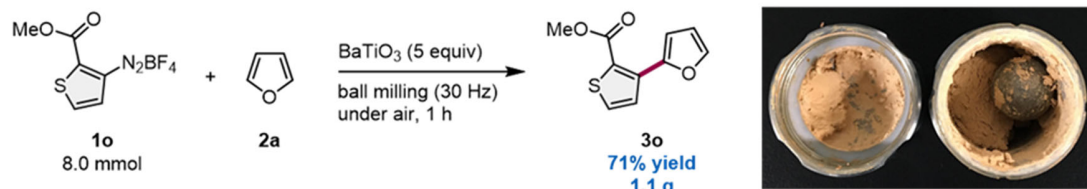


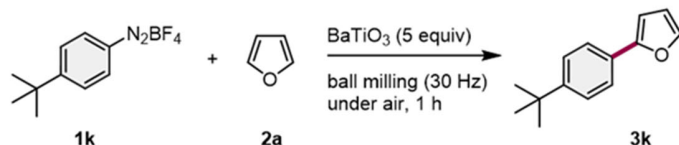
Fig. 3. Scope of the mechano-redox arylation and borylation reactions using aryl diazonium salts. Data for each entry (in bold) are reported as isolated yield percentages. ¹H NMR integrated yields are shown in parentheses. (A) Substrate scope of the mechano-redox arylation of heteroaromatic compounds. (B) Substrate scope of the mechano-redox borylation of aryl diazonium salts. Reactions were performed at 0.3 mmol scale using a stainless-steel milling jar (5 mL) and stainless-steel ball (diameter: 7.5 mm). Arylation conditions: **1** (0.3 mmol), **2** (4.5 mmol), BaTiO₃

(1.5 mmol). Borylation conditions: **1** (0.3 mmol), **4** (0.3 mmol), BaTiO₃ (1.5 mmol), MeCN (0.12 μL/mg). See supplementary materials for details.

A Gram-scale synthesis



B BaTiO₃ recycling experiments



Number of run	Yield (%)	Recovery of BaTiO ₃ (%)
1st run	73	95
2nd run	71	96
3rd run	66	96
4th run	52	98
5th run	43	-

C Direct PAHs functionalization

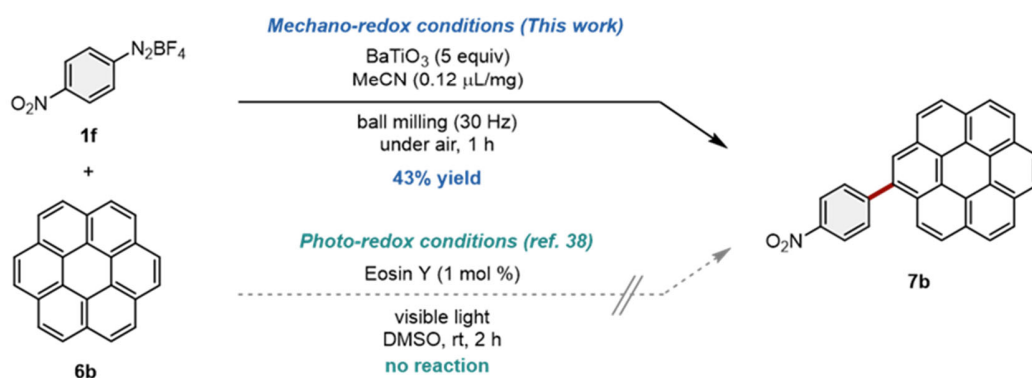
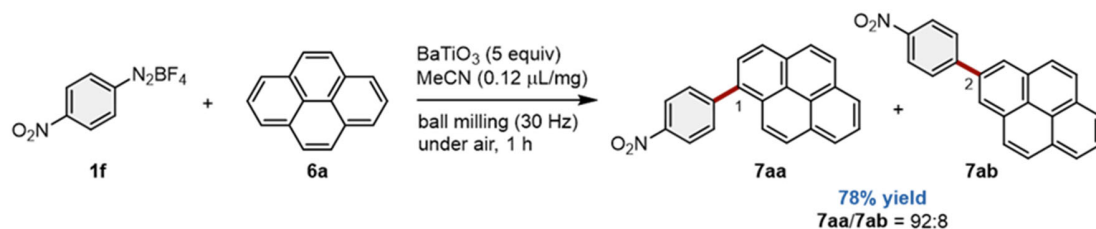


Fig. 4. Exploration of a gram-scale synthesis, catalyst recycling, and the arylation of polyaromatic hydrocarbon compounds. (A) Mechano-redox arylation of **2a** with **1o** on the gram scale using a 25-mL ball-milling jar (picture on the right). (B) BaTiO₃ recycling experiments using **1k** and **2a**. (C) Mechano-redox arylation of the polyaromatic hydrocarbons **6** with **1f**. See supplementary materials for details.

Direct C–H arylation of polycyclic aromatic hydrocarbons (PAHs) has attracted considerable interest (43, 44) on account of their role in organic light-emitting diodes, organic photovoltaics, organic semiconductors, and organic thin-film transistors. With this in mind, we conducted a preliminary investigation of the feasibility of the C–H arylation of PAHs using our mechanoredox approach (Fig. 4C). The reaction of **1f** with pyrene (**6a**) in the presence of BaTiO₃ and a small amount of MeCN as the LAG additive afforded the desired C–H arylation product (**7aa**) in good yield with high regioselectivity (**7aa/7ab** = 92:8). Furthermore, coronene (**6b**) was also arylated in moderate yield under the mechanoredox conditions. When the arylation of coronene (**6b**) was attempted via König's photoredox procedure using Eosin Y, no reaction occurred (37). This was probably due to the low solubility of coronene (**6b**) in the polar solvents required for such photoredox reactions. These results demonstrate the promising potential of the mechanoredox arylation as an operationally simple and mild route to synthesize functionalized PAHs from poorly soluble substrates that are incompatible with photoredox conditions.

We postulated that the mechanoredox C–H arylation and borylation were proceeding via SET events, in which an aryl radical is generated through piezoelectric reduction (Fig. 1C); this assumption is supported by the results of preliminary mechanistic investigations (Fig. 5). When 2,2,6,6-tetramethylpiperidinoxyl (TEMPO) (**8**) was treated with aryl diazonium salt **1a** in the absence of furan (**2a**), the TEMPO-trapped intermediate **9** was obtained (Fig. 5A). Furthermore, the addition of TEMPO (**8**) to a reaction mixture containing **1a**, furan (**2a**), and BaTiO₃ halted the arylation process, and the TEMPO-trapped intermediates **9** and **10** were detected (Fig. 5A). Compound **10** might have been formed through the reaction of TEMPO (**8**) with the intermediate **II** (Fig. 1C), followed by oxidative aromatization by BaTiO₃ or atmospheric oxygen. Overall, the identified compounds suggest that the mechano-redox activation with BaTiO₃ proceeds via a radical pathway.

We used a scanning electron microscopy (SEM) analysis to confirm that the mechanical stimulus provided by ball milling is transferred onto the BaTiO₃ particles under the applied conditions (Fig. 5B) (24). The SEM image of commercially available BaTiO₃ powder shows a regular shape of the BaTiO₃ particles before the reaction (approximate size: <75 μm) [Fig. 5B (i)]. Subsequently, the powder was subjected for 60 min to ball milling at 30 Hz and then analyzed by SEM. The resulting image clearly shows a dramatic distortion of the shape and a decrease in the size of the BaTiO₃ particles [Fig. 5B (ii)]. These results suggest that the mechanical stimulus provided by ball milling is efficiently transferred onto the BaTiO₃ particles, which would result in the generation of localized electrochemical potentials on the surface of the BaTiO₃ particles that can be used for the activation of the aryl diazonium salts.

To investigate whether the friction during ball milling generates a thermal effect, the temperature inside the milling jar during the mechanoredox arylation of **2a** with **1a** was measured using thermography immediately after opening the jar (Fig. 5C). The crude mixtures were prepared under optimized conditions. The obtained image showed that the temperature after arylation in the ball mill was around 30 °C, thus discounting the possibility of thermal activation of the aryl diazonium salts to generate aryl radical species by the heat provided from ball milling.

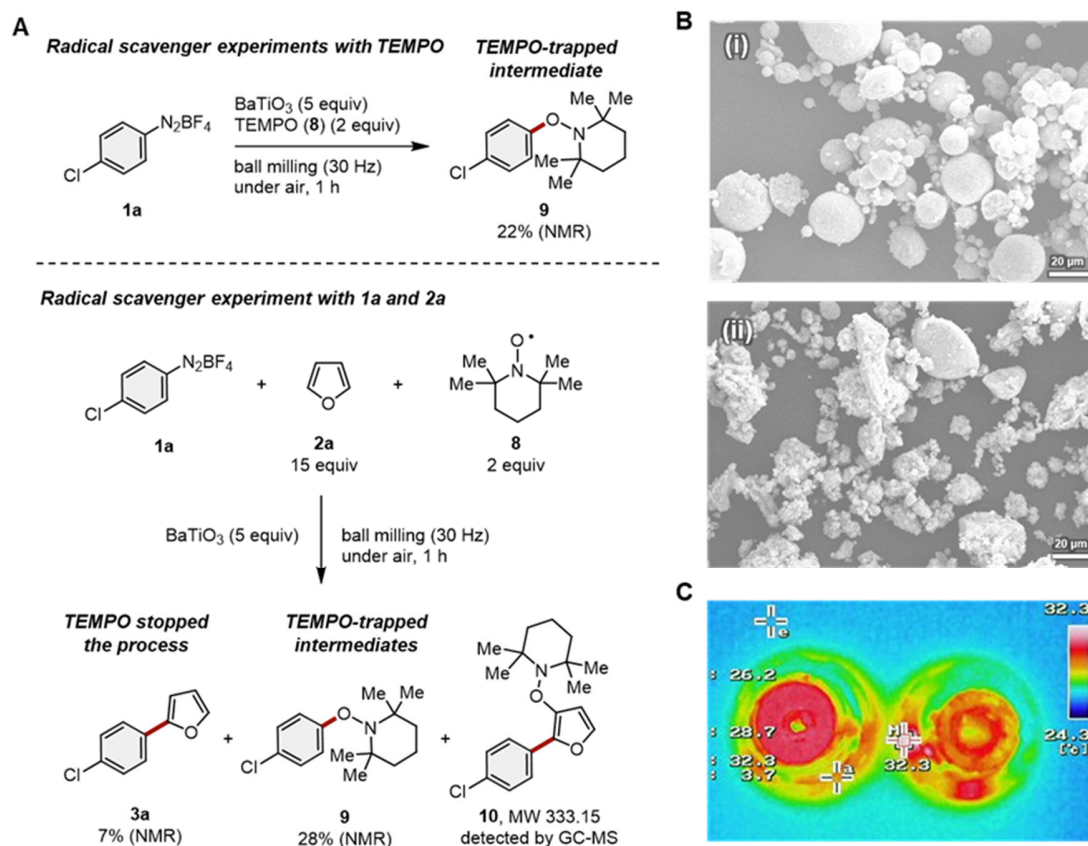


Fig. 5. Mechanistic studies. (A) Radical scavenger experiments. (B) SEM images of BaTiO₃ particles (i) before and (ii) after ball milling (30 Hz; 60 min); scale bars in the TEM images (bottom right): 20 μm. (C) Thermographic image of the milling jar after the mechano-redox arylation of **2a** with **1a**. See supplementary materials for details.

To demonstrate the robustness of the mechano-redox transformations, we conducted the borylation of **1k** with BaTiO₃ in air using a hammer (Fig. S8 and movie S1). First, the reaction mixture was prepared by gentle grinding in a mortar. Subsequently, the mixture was wrapped in a piece of a weighing paper and placed in a zipper-locking plastic bag, followed by striking with a hammer over 200 times. Even under these crude conditions, the mechano-redox borylation product **5i** was obtained in 43% yield as assessed by NMR integration.

The present mechano-redox reactions can be carried out on gram scale without the use of large amounts of dry and degassed organic solvents in air, and do not require special operating conditions. This operational simplicity suggests that the present approach may complement existing photoredox transformations in a practical and environmentally friendly manner. Beyond the immediate benefits of this protocol, our strategy could be applicable to light-sensitive or light-absorbing substrates that cannot be subjected to conventional photo-redox systems.

References and notes:

1. C. Stephenson, T. Yoon, D. W. C. MacMillan, *Visible Light Photocatalysis in Organic Chemistry* (Wiley-VCH, Weinheim, Germany, ed. 1, 2018).
2. C. K. Pier, D. A. Rankic, D. W. C. MacMillan, *Chem. Rev.* **113**, 5322–5363 (2013).
3. N. A. Romero, D. A. Nicewicz, *Chem. Rev.* **116**, 10075–10166 (2016).
- 5 4. C.-S. Wang, P. H. Dixneuf, J.-F. Soulé, *Chem. Rev.* **118**, 7532–7585 (2018).
5. K. L. Skubi, T. R. Blum, T. P. Yoon, *Chem. Rev.* **116**, 10035–10074 (2016).
6. T. Friščić, *J. Mater. Chem.* **20**, 7599–7605 (2010).
7. S.-E. Zhu, F. Li, G.-W. Wang, *Chem. Soc. Rev.* **42**, 7535–7570 (2013).
8. P. Baláž, *Mechanochemistry in Nanoscience and Minerals Engineering* (Springer, 2008).
- 10 9. R. Boulatov, *Polymer Mechanochemistry* (Switzerland, Springer, 2015).
10. S. L. James, C. J. Adams, C. Bolm, D. Braga, P. Collier, T. Friščić, F. Grepioni, K. D. M. Harris, G. Hyett, W. Jones, A. Krebs, J. Mack, L. Maini, A. G. Orpen, I. P. Parkin, W. C. Shearouse, J. W. Steed, D. C. Waddell, *Chem. Soc. Rev.* **41**, 413–447 (2012).
11. G.-W. Wang, *Chem. Soc. Rev.* **42**, 7668–7700 (2013).
- 15 12. J.-L. Do, T. Friščić, *ACS Cent. Sci.* **3**, 13–19 (2017).
13. J. G. Hernández, C. Bolm, *J. Org. Chem.* **82**, 4007–4019 (2017).
14. D. Tan, T. Friščić, *Eur. J. Org. Chem.* 18–33 (2018).
15. J. L. Howard, Q. Cao, D. L. Browne, *Chem. Sci.* **9**, 3080–3094 (2018).
16. J. Andersen, J. Mack, *Green Chem.* **20**, 1435–1443 (2018).
- 20 17. C. Bolm, J. D. Hernández, *Angew. Chem., Int. Ed.* **58**, 3285–3299 (2019).
18. F. Gomollón-Bel, *Chem. Int.* **41**, 12–17 (2019).
19. J. C. Robertson, M. L. Coote, A. C. Bissmber, *Nat. Rev. Chem.* **3**, 290–304 (2019).
20. J. Liang, J. M. Fernández, *J. Am. Chem. Soc.* **133**, 3528–3534 (2011).
- 25 21. P. Dopieralski, J. Ribas-Arino, P. Anjukandi, M. Krupicka, J. Kiss, D. Marx, *Nature Chem.* **5**, 685–691 (2013).
22. H. Yan, F. Yang, D. Pan, Y. Lin, J. N. Hohman, D. Solis-Ibarra, F. H. Li, J. E. P. Dahl, R. M. K. Carlson, B. A. Tkachenko, A. A. Fokin, P. R. Schreiner, G. Galli, W. L. Mao, Z.-X. Shen, N. A. Melosh, *Nature* **554**, 505–510 (2018).
- 30 23. S. Ikeda, T. Takata, M. Komoda, M. Hara, J. N. Kondo, K. Domen, A. Tanaka, H. Hosono, H. Kawazoe, *Phys. Chem. Chem. Phys.* **1**, 4485–4491 (1999).
24. M. Hara, H. Hasei, M. Yashima, S. Ikeda, T. Takata, J. N. Kondo, K. Domen, *Appl. Catal. A-Gen.* **190**, 35–42 (2000).
25. Z. L. Wang, J. Song, *Science* **312**, 242–246 (2006).
26. X. Wang, J. Song, J. Liu, L. Wang, *Science* **316**, 102–105 (2007).

27. Y. Qin, X. Wang, Z. L. Wang, *Nature* **451**, 809–813 (2008).
28. K.-S. Hong, H. Xu, H. Konishi, X. Li, *J. Phys. Chem. Lett.* **1**, 997–1002 (2010).
29. H. Mohapatra, M. Kleiman, A. P. Esser-Kahn, *Nature Chem.* **9**, 135–139 (2017).
30. M. B. Starr, J. Shi, X. Wang, *Angew. Chem., Int. Ed.* **51**, 5962–5966 (2012).
- 5 31. M. B. Starr, X. Wang, *Sci. Rep.* **3**, 2160 (2013).
32. H. Lin, Z. Wu, Y. Jia, W. Li, R.-K. Zheng, H. Luo, *Appl. Phys. Lett.* **104**, 162907 (2014).
33. W. Lv, L. Kong, S. Lan, J. Feng, Y. Xiong, S. Tian, *J. Chem. Technol. Biotechnol.* **92**, 152–156 (2017).
34. M. B. Starr, X. Wang, *Nano Energy* **14**, 296 (2015).
- 10 35. W. Zhenhua, L. Francesca, F. Marco, W. Zongyu, Y. Jianjun, W. Zhanhua, X. Hesheng, K. Matyjaszewski, *ACS Macro Lett.* **8**, 161 (2019).
36. K. Matyjaszewski, *Macromolecules* **45**, 4015 (2012).
37. D. P. Hari, P. Schroll, B. König, *J. Am. Chem. Soc.* **134**, 2958–2961 (2012).
38. J. Yu, L. Zhang, G. Yan, *Adv. Synth. Catal.* **354**, 2625–2628 (2012).
- 15 39. C. P. Andrieux, J. Pinson, *J. Am. Chem. Soc.* **125**, 14801–14806 (2003).
40. J. H. Haeni, P. Irvin, W. Chang, R. Uecker, P. Reiche, Y. L. Li, S. Choudhury, W. Tian, M. E. Hawley, B. Craigo, A. K. Tagantsev, X. Q. Pan, S. K. Streiffer, L. Q. Chen, S. W. Kirchoefer, J. Levy, D. G. Schlom, *Nature* **430**, 758–761 (2004).
41. T. Frišćić, S. L. Childs, S. A. A. Rizvi, W. Jones, *CrystEngComm* **11**, 418–426 (2009).
- 20 42. M. E. Cinar, T. Ozturk, *Chem. Rev.* **115**, 3036 (2015).
43. Y. Segawa, H. Ito, K. Itami, *Nat. Rev. Mater.* **1**, 15002 (2016).
44. Y. Segawa, T. Maekawa, K. Itami, *Angew. Chem., Int. Ed.* **54**, 66–81 (2015).

25 Pls add the rest of the references (from the supplement) here: the full list will be published online.

45. R. Cai, M. Lu, E. Y. Aguilera, Y. Xi, N. G. Akhmedov, J. L. Petersen, H. Chen, X. Shi, *Angew. Chem. Int. Ed.* **54**, 8772–8776 (2015).
46. T. Taniguchi, M. Imoto, M. Takeda, F. Matsumoto, T. Nakai, M. Mihara, T. Mizuno, A. Nomoto, Ogawa, *Tetrahedron* **27**, 4132–4140 (2016).
- 30 47. S. Zhang, Z. Tang, W. Bao, J. Li, B. Guo, S. Huang, Y. Zhang, Y. Rao, *Org. Biomol. Chem.* **17**, 4364–4369 (2019).
48. L. Wang, Z.-X. Wang, *Org. Lett.* **9**, 4335–4338 (2007).
49. W. Su, S. Uragaonkar, P. A. McLaughlin, J. G. Verkade, *J. Am. Chem. Soc.* **126**, 16433–

16439 (2004).

50. N. Morimoto, K. Morioku, H. Suzuki, Y. Nakai, Y. Nishina, *Chem. Commun.* **53**, 7226–7229 (2017).

51. E. Yamamoto, K. Izumi, Y. Horita, H. Ito, *J. Am. Chem. Soc.* **134**, 19997–20000 (2012).

52. B. Wrackmeyer, *Prog. Nucl. Magn. Reson. Spectrosc.* **12**, 227–259 (1979).

53. N. F. Pelz, A. R. Woodward, H. E. Burks, J. D. Sieber, J. P. Morken, *J. Am. Chem. Soc.* **126**, 16328–16329 (2004).

54. C. Kleeberg, L. Dang, Z. Lin, T. B. Marder, *Angew. Chem. Int. Ed.* **48**, 5350–5354 (2009).

55. W. K. Chow, O. Y. Yuen, C. M. So, W. T. Wong, F. Y. Kwong, *J. Org. Chem.* **77**, 3543–3548 (2012).

56. F. Mo, Y. Jiang, D. Qiu, Y. Zhang, J. Wang, *Angew. Chem. Int. Ed.* **49**, 1846–1849 (2010).

57. T. Yamamoto, T. Morita, J. Takagi, T. Yamakawa, *Org. Lett.* **13**, 5766–5769 (2011).

58. M. Beinhoff, W. Weigel, M. Jurczok, W. Rettig, C. Modrakowski, I. Brüdgam, H. Hartl, A. D. Schlüter, *Eur. J. Org. Chem.* 3819 (2001).

Acknowledgments: Funding: This work was supported by the Japan Society for the Promotion of Science (JSPS) through KAKENHI grants 18H03907, 17H06370, 19K15547, and by the JST CREST grant number JPMJCR19R1 as well as by the Institute for Chemical Reaction Design and Discovery (ICReDD), which was established by the World Premier International Research Initiative (WPI), MEXT, Japan. Y. P. thanks the Otsuka Toshimi Scholarship Foundation for a scholarship. We thank D. F. Toste and T. Shimada for advices on the preparation of this manuscript. **Author contributions:** H.I. came up with the original idea; K.K. and H.I. directed the project; K.K. and H.I. designed the experiments; K.K. and Y.P. performed the experiments; A.M. prepared ceramic materials used in this study; K.K. and H.I. wrote the manuscript with feedback from the other authors. **Competing interests:** The authors declare no competing interests; **Data and materials availability:** All data are available in the supplementary materials.

Supplementary Materials:

Materials and Methods

Figures S1 to S9

Tables S1 to S5

Movie S1

References (43-56)

NMR Spectra